Biofilm inhibition by biocompatible poly(ε-caprolactone) nanocapsules loaded with essential oils and their cyto/genotoxicity to human keratinocyte cell line

Magdaléna Kapustová[a†], Andrea Puškárová[a], Mária Bučková[a], Giuseppe Granata[b†], Edoardo Napoli[b], Adriana Annušová[c], Monika Mesárošová[d], Katarína Kozics[d], Domenico Pangallo[a]*, Corrada Geraci[b]*

[a] *Institute of Molecular Biology, Slovak Academy of Sciences, Dúbravská cesta 21, 84551, Bratislava, Slovakia.*

[b] *Istituto Chimica Biomolecolare – Consiglio Nazionale delle Ricerche, Via Paolo Gaifami 18, 95126 Catania, Italy.*

[c] *Institute of Physics, Slovak Academy of Sciences, Dúbravská cesta 9, Sk-84511 Bratislava, Slovakia*

[d] *Cancer Research Institute, Biomedical Research Center, Slovak Academy of Sciences, Dúbravská cesta 9, 84505, Bratislava, Slovakia.*

† These authors contributed equally to this work

*Corresponding author: domenico.pangallo@savba.sk.; corrada.geraci@icb.cnr.it

Abstract

Essential oils (EOs) of *Thymus capitatus* (Th) carvacrole chemotype and *Origanum vulgare* (Or) thymol and carvacrol chemotype were encapsulated in biocompatible poly(ε-caprolactone) nanocapsules (NCs). These nanosystems exhibited antibacterial, antifungal, and antibiofilm activities against *Staphylococcus aureus, Escherichia coli,* and *Candida albicans.* Th-NCs and Or-NCs were more effective against all tested strains than pure EOs and at the same time were not cytotoxic on HaCaT (T0020001) human keratinocyte cell line. The genotoxic effects of EO-NCs and EOs on HaCaT were evaluated using an alkaline comet assay for the first time, revealing that Th-NCs and Or-NCs did not induce DNA damage compared with untreated control HaCaT cells in vitro after 24 h. The cells morphological changes were assessed by label-free live cell Raman imaging. This study demonstrate the ability of poly(ε-caprolactone) nanocapsules loaded with thyme and oregano EOs to reduce microbial and biofilm growth and could be an ecological alternative in the development of new antimicrobial strategies.

Keywords: Antimicrobial, Antibiofilm, Poly(ε-caprolactone) nanocapsule, Essential oils, Label-free Raman imaging

1. Introduction

Biofilm provide the barrier to even small molecule antimicrobial agents affording the suitable support for colonization and development of highly organized communities. This is in part due to their ability to adhere to the surface and develop biofilm, a multilayered structure comprising of bacterial communities embedded within the extracellular hydrated polymeric matrix (Costerton et al., 1995)0. Also because biofilm structure allows bacteria to resist any types of environmental stress including UV, lack of nutrients, and the presence of antimicrobials (Reffuveille et al., 2017)0. Medical devices commonly infected by biofilms include intravenous catheters, vascular prosthesis, prosthetic heart valves, urinary catheters, joint prostheses, cardiac pacemakers, and contact lenses (Han et al., 2017)0. Consequently, searching for effective and biofilm preventing bactericidal agents is deemed necessary in the clinical perspective of antibacterial therapy (Beyth et al., 2015). Designing new generation or derivative of antibiotics is incredibly costly investment process and it wastes much time until it is distinguished in the pharmaceutical production pipelines, however, protection through a smart delivery system can potentiate the bactericidal efficacy of existing antibiotics and adequately address a solution to cease the current progression of resistant bacteria (Shaaban et al., 2017). The failure of existing strategies to treat biofilm-associated infections necessitates the development of an improved drug delivery system and alternative strategies to overcome the limitations of conventional antibiotics including short half-life, low bioavailability, and systemic toxicity (Han et al., 2017). Microorganisms can adhere to various surfaces in food industries, medical equipment, air conditioning units and various indoor and outdoor environment and produce biofilms (Jun et al., 2010; Valeriano et al., 2012). The ability of some essential oils (EOs) to prevent the formation of *Listeria monocytogenes* (de Oliveira et

al., 2010)0 and *Salmonella enterica* (Valeriano et al., 2012) biofilm on stainless steel surfaces has previously been demonstrated.

Staphylococcus aureus is a Gram-positive, ubiquitous bacterial species. *S. aureus* is acknowledged as a key pathogen implicated in industries as well as in the medical domain (Reffuveille et al., 2017). *Escherichia coli* is a Gram-negative bacterium which is a facultative anaerobic in nature. *E. coli*, either pathogenic or of environmental origin, are able to colonize surfaces through production of adhesion determinants and develop as a biofilm, which could result in longer persistence in the environment and in possible reiterated contamination and infection (Castonguay et al., 2006). *Candida albicans* is an opportunistic pathogenic yeast and a its major virulence attribute is ability to form biofilms (Gulati and Nobile, 2016; Lee et al., 2019).

Nanotechnology is an extremely promising way to improve and enhance drug delivery to microbial biofilm. Various antimicrobial agents could be loaded in a wide range of carriers such as mesoporous silica nanoparticles (NPs), dendrimers, polymeric micelles, and lipid-based NPs. The encapsulation allows them to freely circulate in the blood without causing further damages and also better penetration to the biofilm structure (Malaekeh-Nikouei et al., 2020). Several studies have reported on the use of antibiotic-loaded polymeric particles to improve the antimicrobial susceptibility towards biofilms (Birk et al., 2021). Torge et al. (2017) used ciprofloxacin-loaded lipid-core nanocapsules for the treatment *S. aureus* biofilm. Türeli et al. (2017) tested ciprofloxacin-loaded in poly (lactide-co-glycolide) (PLGA) nanoparticles against cystic fibrosis *P. aeruginosa* lung infections. Takahashi et al. (2017) studied of efficacy of clarithromycin-loaded nanocarriers for the treatment of *Staphylococcus epidermidis* biofilm infection disease. Dimer et al. (2020) demonstrate to efficiency PLGA nanocapsules improve the delivery of clarithromycin to kill intracellular *Staphylococcus aureus* and *Mycobacterium abscessus.*In our study, we used essential oils as natural

antimicrobial agents. EOs are volatile phytocomplexes extracted from aromatic plants by distillation. They are very complex mixture of compounds belonging to different chemical classes (hydrocarbons, alcohols, esters, ethers, aldehydes, ketones, phenols), possessing numerous biological activities (Napoli and Ruberto, 2012). Among the many biological activities reported in the literature for essential oils, their antimicrobial effects are well known and have been widely reviewed previously (Bakkali et al., 2008; Schillaci et al., 2013; Napoli et al., 2020). Due to their multi-component nature, the antimicrobial mechanism of EOs is multitarget and up to now, there is no evidence of the occurrence of essential oils resistance. Additionally, EOs could be used to fight multi-drug resistance of pathogenic microorganisms (Bučková et al., 2018; Granata et al., 2018a). Their large-scale industrial application has up to now been limited by the problems linked to the volatility, hydrophobia and degradability of these phytocomplexes (Napoli et al., 2021). EOs are compounds which easily evaporates and/or decomposes during food processing, drug formulation, and preparation of antimicrobial film, etc., owing to direct exposure to heat, pressure, light, or oxygen (Hosseini et al., 2013). There is a growing interest of using essential oils in nanotechnology due to their biological and medical properties, such as bactericidal, virucidal, fungicidal, antiparasitical, insecticidal, analgesic, anti-inflammatory and other properties (Lammari et al., 2020)0.

Nanoencapsulation of EOs represents a viable and efficient approach to increase their physical stability, water solubility, potential antimicrobial and decrease of toxicity, improving bioaccessibility and bioavailability. Compared to large capsule, nanocapsules have higher surface area to volume ratio that represents an important factor for the reactivity. In fact, their subcellular size could favor an enhancement of EOs in water-rich phase or liquid solid interfaces, where the microorganisms are located (Weiss et al., 2009). In particular, the improved penetrative ability of antimicrobial EOs by encapsulation could allow to overcome the microbial biofilm barrier and achieve the eradication of the biofilm (Du et al., 2015).

Numerous microbial antibiofilm agents have been encapsulated in different nanocarriers including solid lipid nanoparticle, liposome, nanostructured lipid carrier, metal or polymeric nanoparticle. Generally, these nanosystems possess enhnaced anti-biofilm activity compared to antimicrobials alone (Malaekeh-Nikouei, 2020).

The discovery of new biodegradable and biocompatible nanosystems with antibiofilm activity is a topic of great interest. In this work we focus our attention on the realization of new eco-friendly nanosystems able to combat microbial biofilm, by using a polymeric nanocarrier loaded with plant EO as natural antibiofilm agents.

Poly(ε-caprolactone) (PCL) is a promising polymer for the development of nanoparticles. PCL is a biodegradable and biocompatible polyester polymer, having a semicrystalline structure with low glass transition temperature *Tg* (- 60°C) and low melting point temperature (60°C). Due to the presence of hydrolysis-unstable aliphatic ester linkage, PCL is biodegraded *in vivo* to low molecular weight non-toxic substances (e.g. 6-hydroxycaproic acid), completely metabolized in the human body (Espinoza et al., 2020). Compared to other polymers, [e.g. polylactid (PLA) and PLGA), PCL biodegrades more slowly and its biodegradation does not generate an acidic environment (Hamoudeh et al., 2006). For this reason, PCL finds various applications including tissue bioengineering, implants and surgical adsobable sutures, wound healing, and antimicrobial and oral vaccine delivery (Benoit et al., 1990; Woodruff and Hutmacher, 2010; Sharifi et al., 2016).

Several studies have been conducted regarding the genotoxic properties of EOs (Ortiz et al., 2016; Puškárová et al., 2017; Shokrzadeh et al., 2017; Kampke et al., 2018; Kozics et al., 2019; Mesic et al., 2021) but only a few studies for nanomaterial containing EOs. Examples of nanomaterial-induced oxidative DNA damage have been reported by some authors and oxidative stress is considered the major action mechanism of nanomaterial genotoxicity (Zijno et al., 2015; Platel et al., 2016).

143 With this in mind, we prepared two PCL-based nanocapsules (NCs) loaded with thyme and
144 oregano essential oils and their antibacterial, antifungal and antibiofilm activity was assayed.
145 The concentrations of nanoencapsulated EOs able to prevent the growth and the biofilm
146 formation of *Staphylococcus aureus, Escherichia coli* and *Candida albicans* were determined.
147 We also report the first in vitro results on the cytotoxic and genotoxic activities of these EO-
148 NCs in human keratinocyte cell line HaCaT (T0020001). The cell morphological changes
149 induced by EOs, NCs and EO-NCs are visualized by label-free Confocal Raman Microscopy
150 imaging.
151
152 **2. Materials and methods**
153
154 **2.1. Essential oils and Nanocapsule characterization**
155 The essential oils and essential oil-loaded nanocapsules (EO-NCs) were obtained and
156 characterized as performed in our previous works (Granata et al., 2018a; Granata et al., 2018b;
157 Avola et al., 2020; Kapustová et al., 2021). Nevertheless, some information such as
158 characterization of essential oil starting material by GC-FID and GC-MS, preparation of EO-
159 NCs, physicochemical characterization of EO-NCs (including encapsulation efficiency (EE)
160 and loading capacity (LC) determinations, particle size, polydispersity, and zeta potential
161 measurements) are briefly described in Supplementary Material (Table S1 and Fig. S1).
162
163 **2.2. Microorganisms and grow conditions**
164 *Staphylococcus aureus* CCM 4223 and *Escherichia coli* CCM 3988 were obtained from the
165 Czech Collection of Microorganisms, Masaryk University (Brno, Czech Republic). Bacterial
166 cultures were subcultured from freezer stocks onto Mueller-Hinton agar (MHA) plates and

incubated at 37 °C overnight. All subsequent liquids subcultures, grown in Mueller-Hinton broth (MHB), were derived from colonies grown from the MHA plates.

Candida albicans SC 5314 (Gillum et al., 1984) was subcultured from freezer stocks onto yeast extract peptone dextrose medium (YPD) agar plates and incubated at 30 °C overnight to generate *C. albicans* yeast for experiments. All subsequent liquid subcultures, grown in YPD broth, were derived from colonies isolated from these plates.

2.3. Cell Culture

The human keratinocyte cell line HaCaT (T0020001) was purchased from AddexBio (San Diego, USA). The cells (HaCaT) were cultivated in Dulbecco's Modified Eagle Medium (DMEM) supplemented with 10% fetal calf serum (FCS) and antibiotics (penicillin 100 U/mL; streptomycin 100 µg/mL). The cells were cultured in a humidified atmosphere of 5% CO_2 at 37°C. The media and chemicals used for cell cultivation were purchased from Gibco BRL (Paisley, UK).

2.4. Minimum inhibitory concentration (MIC), minimum bactericidal concentration (MBC) and minimum fungicidal concentration (MFC)

Microtiter plate assays were performed according to Poaty et al. (2015) with modification to determine the MIC, MBC, and MFC of Th-NCs, Or-NCs and Th-EO, Or-EO against bacteria and yeasts. EOs were diluted with 5% dimethyl sulfoxide (DMSO) to 50 mg/mL. Th-NC (5.7 mg/mL of EO) and Or-NC (5.8 mg/mL of EO) nanosuspensions were diluted in MHB medium for bacteria and in YPD for yeast to working solution with concentration of 5 mg/mL. Next dilutions were performed from working solution in same media to final concentration of 3 to 0.03 mg/mL. The empty NC nanosuspension was prepared as described in Supporting Material and was used as NC antimicrobial activity controls and wells with

192 sterile MHB or YPD as sterility controls. Subsequently, each well was inoculated 100 µL 10^5
193 CFU/mL of the bacteria or yeasts. Microplates were incubated for 18 h at 37 °C. After
194 incubation, in each well 10 µL of 3-(4,5-dimethyl-thiazoyl)-2,5-diphenyltetrazolium bromide
195 (MTT) (5 mg/mL) were added, and the microplates were incubated again for 2 h at 37 °C.
196 Then, 100 µL of detergent (isopropyl alchol and HCl) were added, mixed, and optical density
197 was measured at 540 nm by 800 TS Absorbance Reader (BioTek, Winooski, USA). MIC
198 value was determined at the lowest concentrations of the antimicrobial agent inhibiting
199 bacterial/yeasts growth, MBC and MFC as the lowest concentration of each antimicrobial
200 agent resulting in microbial death.
201
202 **2.5. Microtiter biofilm assay**
203 Biofilms formation was processed as described previously (Hariott and Noverr, 2009) with
204 small modifications. The overnight cultures, grown in broth, were washed twice in sterile
205 phosphate buffer saline (PBS) by centrifugation at 3000 *g* for 5 min at room temperature.
206 Suspension of cells (*S. aureus, E. coli*) was diluted and the optical density at OD 600 was
207 adjusted to 0.5 in the medium by spectrophotometer measurement. *C. albicans* was diluted to
208 final concentration in media on 2×10^6 CFU/mL. 100 µL of microbial suspension was added to
209 the microtiter plate. This plate was incubated 90 minutes at 37 °C. After incubation, the
210 supernatant that contained the non-adhered cells was removed and the well was rinsed 2 times
211 with sterile PBS. EOs were diluted with 5% DMSO to 50 mg/mL. Th-NC (5.7 mg/mL of EO)
212 and Or-NC (5.8 mg/mL of EO) nanosuspensions were diluted in MHB media for bacteria and
213 in YPD for yeast to working solution with concentration of 5 mg/mL. Next dilutions were
214 performed from working solution in same media to final concentration of 0.5 to 0.03 mg/mL.
215 Empty NCs were used as NC antimicrobial activity controls and wells with sterile MHB or
216 YPD as sterility controls. Subsequently, the media and concentration of EO or EO-NCs were

added to the wells containing the adhered cells. The final volume of each well was 200 µL. This plate was incubated 24 h at 37 °C. After incubation, the supernatant was removed and the well was rinsed 2 times with sterile PBS, and 90 µL of media was added to each well. For measurement of the optical density was added 10 µL of MTT (5 mg/mL), and the plate was incubated 2 h at 37 °C. After incubation was added 100 µL of detergent, mixed and optical density was measured at 540 nm by 800 TS Absorbance Reader (BioTek).

2.6. Determination of cytotoxicity

The metabolic activity of EOs, empty NCs, and Th-NCs, Or-NCs was determined by MTT method. Briefly, 2×10^4 cells were seeded in 96-well plates and cultured in complete DMEM medium. Studied compounds (0 – 2.08 mg/mL) were then added, and cells were incubated at 37°C in a 5% CO_2 atmosphere for 24 h. At the indicated time point, the samples were washed with PBS, followed by the incubation with 1 mg/mL of MTT for 4 h. Then, MTT was removed and the formazan crystals were dissolved with dimethyl sulfoxide for 30 min. As a positive control, hydrogen peroxide (300 µM, Sigma-Aldrich) was used. Absorbance at a wavelength of 540 nm was measured using xMark™ Microplate Spectrophotometer (Bio-Rad Laboratories, Inc.) and background absorbance at 690 nm was subtracted.

2.7. Determination of genotoxicity

Exponentially growing cells were pre-incubated in the presence of Th (6.25×10^{-4} – 1.1×10^{-2} mg/mL), Or (3.75×10^{-3} – 6×10^{-2} mg/mL), NCs (1.46×10^{-4} – 2.34×10^{-3} mg/mL), Th-NCs (4.38×10^{-3} – 7×10^{-2} mg/mL), Or-NCs (3.25×10^{-4} – 5.4×10^{-3} mg/mL) or without studied compounds (control) for 24 h. Then the cells were washed, trypsinized, re-suspended in a fresh culture medium and used for testing of the level of DNA lesions by the comet assay. The procedure was used with minor modifications suggested by Singh et al. (1998). Slides

were examined with Zeiss Imager.Z2 fluorescence microscope using the computerized image analysis (Metafer 3.6, Meta Systems GmbH, Altlussheim, Germany). The percentage of DNA in the tail (% of tail DNA) was used as a parameter for measurement of DNA damage (DNA strand breaks). One hundred comets were scored per each sample in one electrophoresis run.

2.8. Confocal Raman Microscopy measurements

1.5×10^5 cells were seeded in 6-well plates and cultured in complete DMEM medium. The next day, cells were pre-incubated in the presence of Th-EO (0.1 mg/mL), Or-EO (0.08 mg/mL), empty NCs (0.0468 mg/mL), Th-NCs (0.004 and 0.1 mg/mL), Or-NCs (0.0219 and 0.00219 mg/mL) or without studied compounds (control) for 24 h. Then the cells were washed and examined with confocal Raman microscopy. Confocal Raman Microscopy (CRM) was applied (Alpha300 R+, WITec, Ulm, Germany) on living cells in PBS (pH=7.4, Oxoid, Basingstoke, UK) using an immersive objective (W Plan-Apochromat 63×, NA=1, Zeiss, Germany). Before measurement the glass slides were gently washed three times in 3 mL of PBS. During measurement they were immersed in 4 mL of PBS solution in individual plastic Petri dishes. The samples were excited at a wavelength and power of 532 nm and 5 mW, respectively (Spectra-Physics Excelsior 532-60 Multi Mode). The Raman spectra were acquired through a 50 µm diameter multimode optical fibre, also acting as a pinhole providing confocality, into a spectrometer (UHTS 300, WITec, Ulm, Germany) equipped with a 600gr/mm grating (blazed at 500 nm) and coupled to an EMCCD camera (Newton DU970N-BV-353, Andor, Belfast, UK). The probing volume is limited to approximately 320 nm and 1000 nm in lateral and transversal directions, respectively. Bright field imaging served to select the scanned areas (individual cells). The obtained spectra were subjected to cosmic ray removal. Subsequently, the Principal Component Analysis (PCA) was applied to reduce the initial hyperspectral data dimensionality and increase the experimental signal to noise ratio.

Finally, the *k*-means clustering method enabled the classification of similar regions (cell components) under individual clusters, based mainly on the presence and ratio of different Raman vibrational peaks from organic molecules in the so called fingerprint spectral region (600 - 1800 rel.cm^{-1}), and in the region of 2700 - 3000 rel.cm^{-1}, where vibrational peaks from lipids and proteins manifest as well (Shipp et al., 2017).

2.9. Statistical analysis

The data are given as means of 3 experiments ± one standard deviation (SD). The differences between the given groups were tested for statistical significance using Student's t-test (*$p < 0.05$; **$p < 0.01$; ***$p < 0.001$). Because the antibacterial activity datasets were normally distributed, the independent samples t-test was performed to test for significant differences between groups.

3. Results

3.1. Antimicrobial activities of EO-NCs and pure EOs

The MICs, MBCs, MFCs of Th-NCs, Or-NCs along with pure EOs of *Thymus capitatus* and *Origanum vulgare* against *S. aureus, E. coli, C. albicans* are summarized in Table 1. From these results, we observed that MIC and MBC values of EO-NCs against *E. coli* were twelve or sixteen folds lower than values of pure EOs. The MIC of Th-EO and Or-EO against *E. coli* was reduced from 2 mg/mL to 0.125 mg/mL by both EO-NCs. The MIC of EO-NCs against *S. aureus* was 0.5 mg/mL, whereas MIC against *E. coli* and *C. albicans* was 0.125 mg/mL. The MIC, MBC values of EO-NCs against *S. aureus* were two or four folds lower than values of pure EOs whereas values of EO-NCs against *C. albicans* were eight-fold lower. These results indicate that EO-NCs have the bactericidal and fungicidal activities at least at one-fold

292 higher than MIC on tested strains. On the other hand MIC of EO-NCs were four-sixteen fold
293 lower than it was observed in case of EOs. At the same time, no antimicrobial effects were
294 determined by empty NCs against all microorganisms.
295
296 **3.2. Biofilm inhibitory activity**
297 In this study, Th-NCs, Or-NCs, pure NCs and Th-EO, Or-EO were evaluated for their biofilm
298 inhibitory activity in microtitre plates at sub MIC concentrations depending on the determined
299 MIC of each isolate. The inhibition of biofilm growth by Th-NCs, Or-NCs was confirmed at
300 tested MIC and two sub MIC concentrations ranging from 0.5 to 0.125 mg/mL for *S. aureus*
301 (Fig. 1A), from 0.125 to 0.03 mg/mL for *E. coli* (Fig. 1B) and *C. albicans* (Fig. 1C). As
302 shown in Fig. 1, sub MIC concentrations Th-NCs and Or-NCs for *S. aureus* and *E. coli*
303 resulted in significant inhibition of biofilm formation (*$p<0.05$, **$p<0.01$, ***$p<0.001$)
304 compared to control untreated samples. However, for *C. albicans* (Fig. 1C), no significant
305 reduction was observed for Th-NCs (0.03 and 0.06 mg/mL) and for Or-NCs (0.03 mg/mL),
306 compared to the control untreated cultures. On the other hand, sub MIC of Or-NCs (0.06
307 mg/mL) showed viability of cells of *C. albicans* as significant result (*$p<0.05$). The data of *S.*
308 *aureus* cell biofilm inhibition at 0.25 and 0.125 mg/mL of Th-NCs were as follows 91.1% and
309 52.9% and 0.25 and 0.125 mg/mL of Or-NCs revealed 75% and 43% inhibition, respectively.
310 The biofilm inhibition of data for *E. coli* at 0.06 and 0.03 mg/mL of Th-NCs were as follows:
311 58.27% and 51.01% and Or-NCs (0.06 and 0.03 mg/mL) followed the order: 38.81%, 27.88%
312 inhibition. Sub MICs of Or-NCs (0.06 mg/mL) showed 25.95% biofilm inhibition of cells of
313 *C. albicans*. The results clearly revealed the biofilm inhibiting potential of Th-NCs, Or-NCs.
314 The inhibition of biofilm growth by Th-EO, Or-EO ranging from 2 to 0.125 mg/mL for *S.*
315 *aureus* (Fig. 1A) and *E. coli* (Fig. 1B) and from 1 to 0.125 mg/mL for *C. albicans* (Fig. 1C)
316 which were higher in comparison to MIC and sub MIC concentations of Th-NCs, Or-NCs.

317 Sub MIC concentrations of Th-EO showed no significant inhibition of biofilm formation for
318 all tested isolates. Sub MIC concentrations of Or-EO revealed no significant antibiofilm effect
319 for *C. albicans*. Tested Or-EO (0.25 mg/mL) showed 40% (***$p<0.001$) inhibition of biofilm
320 formation for *E. coli* in comparison to untreated cells. The results of biofilm inhibition at 1
321 and 0.5 mg/mL of Or-NCs showed 89% and 75.7% inhibition for *S. aureus*. In our study Th-
322 NCs, Or-NCs were more effective against biofilms than EOs.
323 The data of antibiofilm activity against *S. aureus, E. coli* and *C. albicans* revealed the biofilm
324 inhibiting potential Th-NCs, Or-NCs. Inhibition of biofilm formation was in a dose related
325 manner. The results show that Th-NCs and Or-NCs had the antibiofilm effect already at low
326 concentration of 0.03 mg/mL.
327
328 **3.3. Cytotoxic and DNA-damaging effects of EOs, NCs and EO-NCs**
329 The cytotoxic effect of EOs and Th-NCs, Or-NCs on HaCaT cells was evaluated by MTT
330 assay in the concentration range 0 – 2.08 mg/mL. The results are summarized in Figure 2. The
331 following IC_{50} values (median inhibitory concentrations that cause approximately 50% cell
332 death) have been determined: 0.044 mg/mL for Or-NCs; 0.0625 mg/mL for NCs; 0.093
333 mg/mL for Or-EO; 0.114 mg/mL for Th-NCs; 0.176 mg/mL for Th-EO.
334 Further studies aimed at the genotoxic effects of EOs and Th-NCs, Or-NCs were assessed at
335 $IC_{\sim 10\text{-}40}$. The level of DNA strand breaks induced in HaCaT cells by studied compounds was
336 determined by the Comet assay (SCGE). For the induction of DNA single strand breaks in
337 HaCaT cells, H_2O_2 at a concentration of 500 μM was selected (determined by SCGE, data not
338 shown) and further used as a positive control. The H_2O_2-induced DNA damage (percentage of
339 DNA in the tail) was about 50%. Five non-genotoxic concentrations for each EO and Th-NCs,
340 Or-NCs were selected for the Comet assay (Fig. 2). Studied compounds did not induce DNA
341 damage compared with untreated control HaCaT cells (Fig. 3).

342

343 **3.4. Label-free Raman imaging of cell morphology changes induced by EOs, NCs and**
344 **EO-NCs**

345 HaCaT cells were subjected to CRM analysis after 24 h incubation with Th-NCs, Or-NCs at
346 both low (non-cytotoxic) and high concentrations (Th-NCs: 0.004 and 0.1 mg/mL; Or-NCs:
347 0.00219 and 0.0219 mg/mL), and with Th-EO, Or-EO and empty NCs at high concentrations
348 (Th-EO: 0.1 mg/mL; Or-EO: 0.088 mg/mL; NCs: 0.0468 mg/mL). As control samples,
349 HaCaT cells without additives were imaged (control). Figure 4 presents bright field images of
350 scanned HaCaT cells from samples incubated with EO-NCs at high concentrations and the
351 resulting false-colored images after PCA and cluster analysis with corresponding Raman
352 spectra. Figure 5 displays the case of cells incubated with EO-NCs at non-cytotoxic
353 concentrations together with the CRM results for control cells. Individual cell components are
354 differentiated: membrane, intracellular matrix, nucleus, organelles and lipo-protein
355 aggregates. The color code for false-colored images and associated graphs is the same. For
356 more clarity, not all corresponding spectra are shown on the graphs (shades of individual
357 colors correspond to slightly different spectral signatures in individual clusters). The wide
358 peak at around 3300 rel.cm^{-1}, common in every spectra, is related to the OH stretching modes
359 of water (the OH bending modes of water are observed around 1600 rel.cm^{-1}, see spectrum of
360 „extracellular matrix“). A significant difference in the case of incubation with high
361 concentrations of EO-NCs (Fig. 4) with regard to control samples (Fig. 5), are the lipo-protein
362 aggregates in the intracellular space for the former case. They are easily distinguishable, as
363 for all other cell compartments the CH_3 symmetric stretch vibrational mode of proteins
364 dominates in this spectral region. Figure 6 displays examples of CRM false-colored images of
365 HaCaT incubated with NCs, Th-EO, Or-EO at high concentrations. These latter
366 measurements allowed to ascertain the morphological changes of HaCaT without considering

the combined effects of EOs and NCs. The lipo-protein aggregates are present likewise, however in reduced numbers and sizes. It indicates, that the cytotoxic effect on HaCaT in the case of high concentrations of EO-NCs can be a synergistic one caused by both EOs and NCs.

4. Discussion

The physicochemical characteristics of PCL nanoparticles loaded with essential oils of thyme and oregano are shown in fig. S1. The z-average diameters of TC-NC and OV-NC are 198 nm and 200 nm, respectively. Furthermore, the EO-NCs showed unimodal size distribution curves and low PDI values (Figure S1). The nanosuspensions exhibited a negative zeta potential and no aggregation and flocculation phenomena were observed. This is attributable to the Tween 80 covering the polymeric wall of the nanocapsules, that is able to stabilize them in solution by steric hindrance. The percentages of EE and LC, (84% and 52% for the TC-NC and 80% and 51% for the OV-NC), calculated as reported in the supplementary material, are promising for a future scaling-up in the preparation of these systems.

The antimicrobial and antibiofilm activities of Th-NCs, Or-NCs along with pure EOs and empty NCs were evaluated against bacterial strains and yeasts which are able to form biofilm. Before performing the studies to determine the antibiofilm activity, the antimicrobial assays (MIC and MBC) were performed to confirm the *S. aureus*, *E. coli* and *C. albicans* susceptibility to the nanosuspensions of Or-NCs, Th-NCs, NCs, and pure EOs. Similarly to what was reported in our previous works (Granata et al., 2018a; Kapustová et al., 2021) antimicrobial activity of the thyme and oregano essential oil encapsulated in poly(ε-caprolactone) was higher than the corresponding pure essential oils, highlighting the effectiveness of the nanoencapsulation strategy in improving the delivery of nanoencapsulated EOs. Both Th-NCs and Or-NCs showed the lowest MIC values for *C. albicans* and *E. coli*

(0.125 mg/mL) while highest for *S. aureus* (0.5 mg/mL). Contrary to what was expected, the gram negative bacterial strain (*E. coli*) was more sensitive than the gram positive strain (*S. aureus*). This could be attributed to the remarkable variety and versatility of the microbial strain in the treatment with nanoparticles.

It is noteworthy that in addition to our aforementioned works, only one article on the antimicrobial activity of EOs encapsulated in polycaprolactone-based nanocapsules is reported in the literature. In this article the authors evaluated the antibacterial activity of PCL nanocapsules loaded with *Cymbopogon martinii* essential oil against *Staphylococcus aureus* and *Escherichia coli* by agar diffusion methods (Jummes et al., 2020).

Differently, numerous works concerning antimicrobial and/or antibiofilm activity of different polymer nanosystems containing essential oils have been reported in the literature and and some examples are shown below. Unfortunately, the use of different methods to determine the antimicrobial activity, the diversity of the essential oils loaded into the nanocapsules together with the different type of polymer used, do not allow easy comparison of the results obtained from different polymeric nanosystems with antimicrobial activity.

Spherical nanocapsules of cellulose acetate contening essential oils of peppermint, cinnamon and lemongras, prepared by solvent/antisolvent technique, showed good antimicrobial effect against *P. aeruginosa, S. aureus*, *E. coli*, and *C. albicans* with MIC values 0.25%, 0.125%, 0.06%, 0.031%, respectively. The different nanoencapsulated EOs also exhibited good antibiofilm activity and cinnamon nanocapsules were more effective in eradicating the microbial biofilm, especially against *C. albicans* (Liakos et al., 2018).

Essential oil of *Mentha piperita* entrapped into chitosan nanoparticle, prepared by sol-gel method, showed at 0.05 mg/mL ability to inhibit the biofilm of *Streptococcus mutans* associated with dental plaque (Ashrafi et al., 2019).

Liakos et al. (2016) also reported the synthesis of functional nanocapsules of polylactic acid-lemongrass essential oil with good antimicrobial and antibiofilm activity against *P. aeruginosa*, *E. coli* and *C. albicans*. For all microorganisms the MIC value was 0.25% and the highest antibiofilm effect was observed for *C. albicans* and *E. coli*.

In the present study, Th-NCs, at both concentrations 0.06 and 0.03 mg/mL, demonstrated the ability to prevent biofilm formation of *E. coli* and they did not display cytotoxicity. The lowest tested concentration of Th-NCs (0.03 mg/mL) showed 51.01% biofilm inhibition for *E. coli* cells. Considering *S. aureus* and *C. albicans*, their biofilm formation was inhibited by the concentration 0.125 mg/mL of Th-NCs that is very close to the value 0.114 mg/mL representing the no cytotoxic concentraction of these nanocapsules.

The Or-NCs at concentration 0.03 mg/mL were able to inhibit the *E. coli* biofilm formation without showing cytotoxicity too. At the same time, the control nanoparticles showed no activity on the bacterial and fungal growth, highlighting that the antimicrobial effects were only obtained from the essential oils encapsulated in polymer-based nanocapsules itself. Th-NCs (0.03 mg/mL) showed the ability to inhibit the biofilm of *E. coli* at lower concentration than it was demonstrated in the previous study by Ashrafi et al., 2019, when they tested chitosan nanoparticles with essential oil from *Mentha piperita* at concentration 0.05 mg/mL against to *Streptococcus mutans* biofilm. Much greater amounts of pure essential oils were needed to inhibit biofilm formation and the Or-EO were more effective than Th-EO in preventing biofilm formation. This could be attributed to the different EO composition in bioactive substances, its physicochemical characteristics and above all to the complex mechanism of action involved in the inhibition of microbial biofilm. As expected, no antibiofilm effect was observed for empty NCs. In light of these results, we reported for the first time the ability to inhibit biofilm formation of three severe pathogenic microorganisms by using two effective nanostructured systems, based on polycaprolactone polymer containing

441 essential oils of oregano and thyme. The biodegradability and biocompatibility of the
442 polymeric carrier (PCL) together with bioactive natural compounds (EOs) make these
443 nanosystems as eco-friendly antibiofilm agents for potential applications in the medical, food
444 and environmental fields.
445 Encapsulation can reduce the loss of activity of the active compounds. On the other hand, it
446 has been found that high concentrations of some essential oils and nanoparticles contributed
447 to tumor development and other harmful changes in the body (Maistro et., 2010). Therefore, it
448 needs to be verified the potential risk of EOs/NPs to human health. In this study we aimed to
449 evaluate the biosafety of the Th-EO, Or-EO as well as of the respective prepared polymer-
450 based nanocapsules (Th-NCs and Or-NCs) and to compare their biological effects on human
451 normal keratinocyte cell line HaCaT. The cytotoxic effect of Th-EO, Or-EO, Th-NCs and Or-
452 NCs was determined by the MTT assay. The results showed that the 24 h treatment of studied
453 cells with Or-EO, Th-EO, Or-NCs and Th-NCs affected cell viability in a dose-dependent
454 manner. Studied compounds exhibited variable potencies (IC_{50}) according to the following
455 sequence: Or-NCs < Or-EOs < Th-NCs < Th-EO. Results showed that thyme encapsulated in
456 polymer-based nanocapsules (Th-NCs) was safer on HaCaT cell line compared to oregano
457 encapsulated in polymer-based nanocapsules (Or-NCs). In particular, IC_{50} values obtained for
458 Th-NCs 0.114 mg/mL which is ~2.6-fold higher than those obtained for Or-NCs (0.044
459 mg/mL). Result showed that encapsulation of EOs increased cytotoxicity of pure studied
460 essential oils. Results obtained in this study are in very good correlation with those published
461 by Carbone et al. 2018. They found that mediterranean EOs loaded-NLC (nanostructured lipid
462 carriers), induce an increase in the ability of the EO in reducing the RAW 264.7 (murine
463 macrophage), HaCaT, A431 (human epidermoid carcinoma) cells viability when it was
464 encapsulated in the NLC structure (Carbone et al., 2018). Al-Otaibi et al. (2018) have studied
465 the effect of NEs (nanoemulsions)-based EOs on the viability HeLa and MCF-7 cells. Our

findings are in agreement with studies which previously confirmed that the cytotoxicity of the EOs were enhanced when included in different nanodelivery systems (Periasamy et al., 2016; Farshi et al., 2017; Le Kim et al., 2017; Milhomem-Paixão et al., 2017; Pereira et al., 2017; Khan et al., 2018). The level of DNA strand breaks induced in HaCaT cells by the studied EOs and EO-NCs was determined by the comet assay. The select concentrations of EOs and EO-NCs, NCs for comet assay were not cytotoxic. The treatment with studied compounds did not induce any significant increase in DNA strand breaks compared to the untreated control cells. These results for EOs are in very good correlation with our previous study, where Or-EO and Th-EO, similarly, did not induce DNA damage in the HEL 12469 cells (Puškárová et al., 2017). Nevertheless, our studied empty NCs did not induce DNA damage in either tested cells at non-cytotoxic concentrations. However, a direct measurement of DNA damage as an element of nanomaterial testing is highly justified because, as shown by Zijno et al. (2015) some nanomaterials may potentiate DNA lesions by disturbing DNA repair machinery. Karabasz et al. (2018; 2019) demonstrated that the nanomaterials (six-layer negatively charged PGA-terminated nanocapsules (NC6)-PGA and five-layer PEGylated nanocapsules (NC5-PEG)) neither decreased viability, nor caused oxidative stress, nor DNA damage in the human cells of hepatic origin, HepG2 cell line. Dalcin et al. (2019) found that the highest concentrations of NC-E (Eudragit RS100® nanocapsules) induced a decrease in cell viability and increased DNA damage. Furthermore, no cytogenotoxicity was demonstrated for the NC-DMY (nanocapsules-dihydromyricetin), since it did not decrease cell viability, as well as did not induce DNA damage (Dalcin et al., 2019). This is in very good correlation with our results. Therefore, our data suggest the *in vitro* safety of these nanoparticles.

Finally, CRM imaging of HaCaT cells showed the existence of lipo-protein aggreagates inside the cells, after applying high concentrations of EOs, NCs and EO-NCs for a 24 h incubation time. Lipid-rich protrusions are a response of cells to stress environment, as was reported

491 before by Huang et al. (2020)0 in their study on human pancreatic cancer cells by Stimulated
492 Raman Scattering (SRS) imaging cytometry. Lipid aggregates manifest themselves as
493 intensive Raman peaks at 2845 and 2880 rel.cm^{-1} (Shipp et al., 2017; Bugárová et al., 2020)0.
494 At low concentrations of EO-NCs, and in control cells without additives, lipo-protein
495 aggregates were not found. This is in consistence with the study of cytotoxicity, which was
496 found to be concentration dependent. CRM imaging of live cells presents a non-disruptive
497 label-free method in cell biology studies (Klein et al., 2012; Shmith et al., 2016; da Costa et
498 al., 2019). In our group we successfully employed this technique previously for the
499 localization of nanoconjugates within cancer and healthy cells (Sohová et al., 2018; Bugárová
500 at al., 2020; Kálosi et al., 2020). In the present paper, CRM measurements were used for the
501 first time to assess the morphological changes on HaCaT cell line after application of EOs,
502 NCs, and EO-NCs.
503

504 **5. Conclusion**

505 Biofilm-associated microorganisms are a serious problem not only in hospitals but also in
506 food industries and various indoor and outdoor environments. This is the first study that
507 determined the antibiofilm effect of essential oils of *Thymus capitatus* and *Origanum vulgare*
508 encapsulated in polymer-based nanocapsules against *S. aureus, E. coli,* and *C. albicans*
509 biofilms. This study allowed a first assessment of the cytotoxic and genotoxic activities of Th-
510 NCs, Or-NCs in human keratinocyte cell line HaCaT (T0020001). Label-free live cell Raman
511 imaging confirmed morphological alterations concerning control cell cultures in the case of
512 high concentration EOs, NCs, and EO-NCs.
513 The data presented in this study shows that the nanoencapsulation of essential oils increases
514 the antimicrobial and antibiofilm effect of thyme and oregano essential oils. Th-NC and Or-
515 NC nanosuspensions showed antibiofilm activity, against *E. coli*, at low concentrations and no

cytotoxic activity against HaCaT human keratinocyte cells at the same tested concentrations. These ecofriendly nanosystems could be an ecological alternative in the development of new antimicrobial and antibiofilm strategies for applications in different fields including medicine, food and environmental

CRediT authorship contribution statement

Conceptualization, C.G. and D.P.; methodology, G.G., A.P., M.B., K.K., A.A., M.M.; formal analysis, G.G., E.N., M.K., K.K., A.A., M.M.; investigation, G.G., E.N., M.K., A.P., M.B., K.K., A.A., M.M.; data curation, E.N., M.K., A.P., M.B., K.K., A.A.; writing—original draft preparation, C.G., E.N., G.G., M.K., A.P., D.P.; writing—review and editing, C.G., D.P.; visualization, G.G., M.K.; supervision, C.G., D.P. project administration, C.G., D.P.; funding acquisition, MB, KK.

Declaration of competing interest

The authors declare that they have no known competing financial interests or personal relationships that could have appeared to influence the work reported in this paper.

Acknowledgements

This work was supported by VEGA Agency with the projects 2/0059/19 and 2/0055/20.

References

Al-Otaibi, W. A., Alkhatib, M. H., Wali, A. N., 2018. Cytotoxicity and apoptosis enhancement in breast and cervical cancer cells upon coadministration of mitomycin C and essential oils in nanoemulsion formulations. Biomed Pharmacother. 106, 946-955. https://doi.org/10.1016/j.biopha.2018.07.041.

Ashrafi, B., Rashidipour, M., Marzban, A., Soroush, S., Azadpour, M., Delfani, S., Ramak, P., 2019. Mentha piperita essential oils loaded in a chitosan nanogel with inhibitory effect on biofilm formation against S. mutans on the dental surface. Carbohydr. Polym. 212, 142-149. https://doi.org/10.1016/j.carbpol.2019.02.018.

Avola, R., Granata, G., Geraci, C., Napoli, E., Graziano, A. C. E., Cardile, V., 2020. Oregano (Origanum vulgare L.) essential oil provides anti-inflammatory activity and facilitates wound healing in a human keratinocytes cell model. Food Chem. Toxicol. 144, 111586. https://doi.org/10.1016/j.fct.2020.111586.

Bakkali, F., Averbeck, S., Averbeck, D., Idaomar, M., 2008. Biological effects of essential oils – A review. Food Chem Toxicol. 46, 446-475. https://doi.org/10.1016/j.fct.2007.09.106.

Benoit, M. A., Baras, B., Gillard, J., 1999. Preparation and characterization of protein-loaded poly(ε-caprolactone) microparticles for oral vaccine delivery. Int. J. Pharm. 184, 73-84. https://doi.org/10.1016/S0378-5173(99)00109-X.

Beyth, N., Houri-Haddad, Y., Domb, A., Khan, W., Hazan, R., 2015. Alternative Antimicrobial Approach: Nano-Antimicrobial Materials. Evid Based Complement Alternat Med Title. 2015, https://doi.org/10.1155/2015/246012.

Birk, S. E., Boisen, A., Nielsen, L. H., 2021. Polymeric nano-and microparticulate drug delivery systems for treatment of biofilms. Adv. Drug Deliv. Rev., 174, 30-52. https://doi.org/10.1016/j.addr.2021.04.005

Bučková, M., Puškárová, A., Kalászová, V., Kisová, Z., Pangallo, D., 2018. Essential oils against multidrug resistant gram-negative bacteria. Biologia. 73, 803-808. https://doi.org/10.2478/s11756-018-0090-x.

Bugárová, N., Annušová, A., Bodík, M., Šiffalovič, P., Labudová, M., Kajanová, I., ... Omastová, M., 2020. Molecular targeting of bioconjugated graphene oxide nanocarriers revealed at a cellular level using label-free Raman imaging. Nanomedicine. 30, 102280. https://doi.org/10.1016/j.nano.2020.102280.

Carbone, C., Martins-Gomes, C., Caddeo, C., Silva, A. M., Musumeci, T., Pignatello, R., ... Souto, E. B., 2018. Mediterranean essential oils as precious matrix components and active ingredients of lipid nanoparticles. Int. J. Pharm. 548, 217-226. https://doi.org/10.1016/j.ijpharm.2018.06.064.

Castonguay, M. H., Van der Schaaf, S., Koester, W., Krooneman, J., Van der Meer, W., Harmsen, H., Landini, P., 2006. Biofilm formation by Escherichia coli is stimulated by synergistic interactions and co-adhesion mechanisms with adherence-proficient bacteria. Res. Microbiol. 157, 471-478. https://doi.org/10.1016/j.resmic.2005.10.003.

Costerton, J. W., Lewandowski, Z., Caldwell, D. E., Korber, D. R., Lappin-Scott, H. M., 1995. Microbial biofilms. Annu. Rev. Microbiol. 49, 711-745. https://doi.org/10.1146/annurev.mi.49.100195.003431.

da Costa, S. G., Richter, A., Schmidt, U., Breuninger, S., Hollricher, O., 2019. Confocal Raman microscopy in life sciences. Morphologie. 103, 11-16. https://doi.org/10.1016/j.morpho.2018.12.003.

583 Dalcin, A. J. F., Vizzotto, B. S., Bochi, G. V., Guarda, N. S., Nascimento, K., Sagrillo, M. R.,
584 ... Gomes, P., 2019. Nanoencapsulation of the flavonoid dihydromyricetin protects
585 against the genotoxicity and cytotoxicity induced by cationic nanocapsules. Colloids
586 Surf. B. 173, 798-805. https://doi.org/10.1016/j.colsurfb.2018.10.066.
587 de Oliveira, M. M. M., Brugnera, D. F., das Graças Cardoso, M., Alves, E., Piccoli, R. H.,
588 2010. Disinfectant action of Cymbopogon sp. essential oils in different phases of
589 biofilm formation by Listeria monocytogenes on stainless steel surface. Food
590 Control. 21, 549-553. https://doi.org/10.1016/j.foodcont.2009.08.003.
591 Dimer, F. A., de Souza Carvalho-Wodarz, C., Goes, A., Cirnski, K., Herrmann, J., Schmitt,
592 V., ... Lehr, C. M., 2020. PLGA nanocapsules improve the delivery of clarithromycin
593 to kill intracellular *Staphylococcus aureus* and *Mycobacterium abscessus*.
594 Nanomedicine 24, 102125. https://doi.org/10.1016/j.nano.2019.102125
595 Du, J., Bandara, H. M. H. N., Du, P., Huang, H., Hoang, K., Nguyen, D., ... Smyth, H. D.,
596 2015. Improved Biofilm Antimicrobial Activity of Polyethylene Glycol Conjugated
597 Tobramycin Compared to Tobramycin in Pseudomonas aeruginosa Biofilms. Mol.
598 Pharm. 12, 1544-1553. https://doi.org/10.1021/mp500846u.
599 Espinoza, S. M., Patil, H. I., San Martin Martinez, E., Casañas Pimentel, R., Ige, P. P., 2020.
600 Poly-ε-caprolactone (PCL), a promising polymer for pharmaceutical and biomedical
601 applications: Focus on nanomedicine in cancer. Int. J. Polym. Mater. 69, 85-126.
602 https://doi.org/10.1080/00914037.2018.1539990.
603 Farshi, P., Tabibiazar, M., Ghorbani, M., Hamishehkar, H., 2017. Evaluation of Antioxidant
604 Activity and Cytotoxicity of Cumin Seed Oil Nanoemulsion Stabilized by Sodium
605 Caseinate- Guar Gum. Pharm. Sci. 23, 293-300. https://doi.org/10.15171/PS.2017.43.
606 Gillum, A. M., Tsay, E. Y., Kirsch, D. R., 1984. Isolation of the Candida albicans gene for
607 orotidine-5′-phosphate decarboxylase by complementation of S. cerevisiae ura3 and E.
608 coli pyrF mutations. Mol. Gen. Genet. 198, 179-182.
609 https://doi.org/10.1007/BF00328721.
610 Granata, G., Consoli, G. M., Nigro, R. L., Geraci, C., 2018b. Hydroxycinnamic acids loaded
611 in lipid-core nanocapsules. Food Chem. 245, 551-556.
612 https://doi.org/10.1016/j.foodchem.2017.10.106.
613 Granata, G., Stracquadanio, S., Leonardi, M., Napoli, E., Consoli, G. M. L., Cafiso, V., ...
614 Geraci, C., 2018a. Essential oils encapsulated in polymer-based nanocapsules as
615 potential candidates for application in food preservation. Food Chem. 269, 286-292.
616 https://doi.org/10.1016/j.foodchem.2018.06.140.
617 Gulati, M., Nobile, C. J., 2016. Candida albicans biofilms: development, regulation, and
618 molecular mechanisms. Microb Infect. 18, 310-321.
619 https://doi.org/10.1016/j.micinf.2016.01.002.
620 Hamoudeh, M., Fessi, H., 2006. Preparation, characterization and surface study of poly-
621 epsilon caprolactone magnetic microparticles. J. Colloid Interface Sci. 300, 584-590.
622 https://doi.org/10.1016/j.jcis.2006.04.024.
623 Han, C., Romero, N., Fischer, S., Dookran, J., Berger, A., Doiron, A. L., 2017. Recent
624 developments in the use of nanoparticles for treatment of biofilms. Nanotechnol. Rev.
625 6, 383-404. https://doi.org/10.1515/ntrev-2016-0054.
626 Harriott, M. M., Noverr, M. C., 2009. Candida albicans and Staphylococcus aureus Form
627 Polymicrobial Biofilms: Effects on Antimicrobial Resistance. Antimicrob Agents
628 Chemother. 53, 3914-3922. https://doi.org/10.1128/AAC.00657-09.
629 Hosseini, S. F., Zandi, M., Rezaei, M., Farahmandghavi, F., 2013. Two-step method for
630 encapsulation of oregano essential oil in chitosan nanoparticles: Preparation,
631 characterization and in vitro release study. Carbohydr. Polym. 95, 50-56.
632 https://doi.org/10.1016/j.carbpol.2013.02.031.

Huang, K. C., Li, J., Zhang, C., Tan, Y., Cheng, J. X., 2020. Multiplex Stimulated Raman Scattering Imaging Cytometry Reveals Lipid-Rich Protrusions in Cancer Cells under Stress Condition. Iscience. 23, 100953. https://doi.org/10.1016/j.isci.2020.100953.

Jummes, B., Sganzerla, W. G., da Rosa, C. G., Noronha, C. M., Nunes, M. R., Bertoldi, F. C., Barreto, P. L. M., 2020. Antioxidant and antimicrobial poly-ε-caprolactone nanoparticles loaded with Cymbopogon martinii essential oil. Biocatal. Agric. Biotechnol. 23, 101499. https://doi.org/10.1016/j.bcab.2020.101499.

Jun, W., Kim, M. S., Cho, B. K., Millner, P. D., Chao, K., Chan, D. E., 2010. Microbial biofilm detection on food contact surfaces by macro-scale fluorescence imaging. J. Food Eng. 99, 314-322. https://doi.org/10.1016/j.jfoodeng.2010.03.005.

Kálosi, A., Labudová, M., Annušová, A., Benkovičová, M., Bodík, M., Kollár, J., ... Majkova, E., 2020. A bioconjugated MoS2 based nanoplatform with increased binding efficiency to cancer cells. Biomater. Sci. 8, 1973-1980. https://doi.org/10.1039/C9BM01975H.

Kampke, E. H., de Souza Barroso, M. E., Marques, F. M., Fronza, M., Scherer, R., Lemos, M. F., ... Gomes, L. C., 2018. Genotoxic effect of Lippia alba (Mill.) N. E. Brown essential oil on fish (Oreochromis niloticus) and mammal (Mus musculus). Environ. Toxicol. Pharmacol., 59, 163-171. https://doi.org/10.1016/j.etap.2018.03.016.

Kapustová, M., Granata, G., Napoli, E., Puškárová, A., Bučková, M., Pangallo, D., Geraci, C., 2021. Nanoencapsulated Essential Oils with Enhanced Antifungal Activity for Potential Application on Agri-Food, Material and Environmental Fields. Antibiotics. 10, 31. https://doi.org/10.3390/antibiotics10010031.

Karabasz, A., Szczepanowicz, K., Cierniak, A., Bereta, J., Bzowska, M., 2018. In vitro toxicity studies of biodegradable, polyelectrolyte nanocapsules. Int. J. Nanomedicine. 13, 5159-5172. https://doi.org/10.2147/IJN.S169120.

Karabasz, A., Szczepanowicz, K., Cierniak, A., Mezyk-Kopec, R., Dyduch, G., Szczęch, M., ... Bzowska, M., 2019. In vivo Studies on Pharmacokinetics, Toxicity and Immunogenicity of Polyelectrolyte Nanocapsules Functionalized with Two Different Polymers: Poly-L-Glutamic Acid or PEG. Int. J. Nanomedicine. 14, 9587-9602. https://doi.org/10.2147/IJN.S230865.

Khan, I., Bahuguna, A., Bhardwaj, M., Pal Khaket, T., Kang, S. C., 2018. Carvacrol nanoemulsion evokes cell cycle arrest, apoptosis induction and autophagy inhibition in doxorubicin resistant-A549 cell line. Artif Cells Nanomed Biotechnol. 46, 664-675. https://doi.org/10.1080/21691401.2018.1434187.

Klein, K., Gigler, A. M., Aschenbrenner, T., Monetti, R., Bunk, W., Jamitzky, F., ... Schlegel, J., 2012. Label-Free Live-Cell Imaging with Confocal Raman Microscopy. Biophys. J. 102, 360-368. https://doi.org/10.1016/j.bpj.2011.12.027.

Kozics, K., Bučková, M., Puškárová, A., Kalászová, V., Cabicarová, T., Pangallo, D., 2019. The Effect of Ten Essential Oils on Several Cutaneous Drug-Resistant Microorganisms and Their Cyto/Genotoxic and Antioxidant Properties. Molecules. 24, 4570. https://doi.org/10.3390/molecules24244570.

Lammari, N., Louaer, O., Meniai, A. H., Elaissari, A., 2020. Encapsulation of Essential Oils via Nanoprecipitation Process: Overview, Progress, Challenges and Prospects. Pharmaceutics. 12, 431. https://doi.org/10.3390/pharmaceutics12050431.

Le Kim, T. H., Yu, J. H., Jun, H., Yang, M. Y., Yang, M. J., Cho, J. W., ... Nam, Y. S., 2017. Polyglycerolated nanocarriers with increased ligand multivalency for enhanced in vivo therapeutic efficacy of paclitaxel. Biomaterials. 145, 223-232. https://doi.org/10.1016/j.biomaterials.2017.08.042.

Lee, J. H., Kim, Y. G., Khadke, S. K., Yamano, A., Watanabe, A., Lee, J., 2019. Inhibition of biofilm formation by Candida albicans and polymicrobial microorganisms by nepodin

via hyphal-growth suppression. ACS Infect. Dis. 5, 1177-1187. https://doi.org/10.1021/acsinfecdis.9b00033.
Liakos, I. L., Grumezescu, A. M., Holban, A. M., Florin, I., D'Autilia, F., Carzino, R., ... Athanassiou, A., 2016. Polylactic Acid—Lemongrass Essential Oil Nanocapsules with Antimicrobial Properties. Pharmaceuticals. 9, 42. https://doi.org/10.3390/ph9030042.
Liakos, I. L., Iordache, F., Carzino, R., Scarpellini, A., Oneto, M., Bianchini, P., ... Holban, A. M., 2018. Cellulose acetate - essential oil nanocapsules with antimicrobial activity for biomedical applications. Colloids Surf. 172, 471-479. https://doi.org/10.1016/j.colsurfb.2018.08.069.
Maistro, E. L., Mota, S. F., Lima, E. B., Bernardes, B. M., Goulart, F. C., 2010. Genotoxicity and mutagenicity of Rosmarinus officinalis (Labiatae) essential oil in mammalian cells in vivo. Genet Mol Res. 9, 2113-2122. http://dx.doi.org/10.4238/vol9-4gmr857.
Malaekeh-Nikouei, B., Bazzaz, B. S. F., Mirhadi, E., Tajani, A. S., Khameneh, B., 2020. The role of nanotechnology in combating biofilm-based antibiotic resistance. J Drug Deliv Sci Technol. 101880. https://doi.org/10.1016/j.jddst.2020.101880
Mesic, A., Mahmutović-Dizdarević, I., Tahirović, E., Durmišević, I., Eminovic, I., Jerković-Mujkić, A., Bešta-Gajević, R., 2018. Evaluation of toxicological and antimicrobial activity of lavender and immortelle essential oils. Drug Chem Toxicol. 44, 190-197. https://doi.org/10.1080/01480545.2018.1538234.
Milhomem-Paixão, S. S. R., Fascineli, M. L., Muehlmann, L. A., Melo, K. M., Salgado, H. L. C., Joanitti, G. A., ... Grisolia, C. K., 2017. Andiroba Oil (Carapa guianensis Aublet) Nanoemulsions: Development and Assessment of Cytotoxicity, Genotoxicity, and Hematotoxicity. J. Nanomater. 2017. https://doi.org/10.1155/2017/4362046.
Napoli, E. M., Ruberto, G., 2012. Sicilian aromatic plants: from traditional heritage to a new agro-industrial exploitation. Spices: Types, Uses and Health Benefits. Kralis. JF. Ed., 1-56.
Napoli, E., Di Vito, M., 2021. Toward a New Future for Essential Oils. Antibiotics. 10, 207. https://doi.org/10.3390/antibiotics10020207.
Napoli, E., Siracusa, L., Ruberto, G., 2010. New Tricks for Old Guys: Recent Developments in the Chemistry, Biochemistry, Applications and Exploitation of Selected Species from the Lamiaceae Family. Chem biodivers. 17, e1900677. https://doi.org/10.1002/cbdv.201900677.
Ortiz, C., Morales, L., Sastre, M., Haskins, W. E., Matta, J., 2016. Cytotoxicity and Genotoxicity Assessment of Sandalwood Essential Oil in Human Breast Cell Lines MCF-7 and MCF-10A. Evid.-Based Complementary Altern. Med. 2016. https://doi.org/10.1155/2016/3696232.
Pereira, F. G., Marquete, R., Oliveira-Cruz, L., Quintanilha-Falcão, D., Mansur, E., de Lima Moreira, D., 2017. Cytotoxic effects of the essential oil from leaves of Casearia sylvestris Sw. (Salicaceae) and its nanoemulsion on A549 tumor cell line. B. Latinoam Caribe Pl. 16, 506-512. https://www.redalyc.org/articulo.oa?id=85652864006.
Periasamy, V. S., Athinarayanan, J., Alshatwi, A. A., 2016. Anticancer activity of an ultrasonic nanoemulsion formulation of Nigella sativa L. essential oil on human breast cancer cells. Ultrason Sonochem. 31, 449-455. https://doi.org/10.1016/j.ultsonch.2016.01.035.
Platel, A., Carpentier, R., Becart, E., Mordacq, G., Betbeder, D., Nesslany, F., 2016. Influence of the surface charge of PLGA nanoparticles on their in vitro genotoxicity, cytotoxicity, ROS production and endocytosis. J. Appl. Toxicol. 36, 434-444. https://doi.org/10.1002/jat.3247.
Poaty, B., Lahlah, J., Porqueres, F., Bouafif, H., 2015. Composition, antimicrobial and antioxidant activities of seven essential oils from the North American boreal forest.

World J. Microbiol. Biotechnol. 31, 907-919. https://doi.org/10.1007/s11274-015-1845-y.
Puškárová, A., Bučková, M., Kraková, L., Pangallo, D., Kozics, K., 2017. The antibacterial and antifungal activity of six essential oils and their cyto/genotoxicity to human HEL 12469 cells. Sci. Rep. 7, 1-11. https://doi.org/10.1038/s41598-017-08673-9.
Reffuveille, F., Josse, J., Vallé, Q., Gangloff, C. M., Gangloff, S. C., 2017. Staphylococcus aureus Biofilms and their Impact on the Medical Field. The Rise of Virulence and Antibiotic Resistance in Staphylococcus aureus. 11, 187. https://dx.doi.org/10.5772/66380.
Shaaban, M. I., Shaker, M. A., Mady, F. M., 2017. Imipenem/cilastatin encapsulated polymeric nanoparticles for destroying carbapenem-resistant bacterial isolates. J Nanobiotechnology. 15, 1-12. https://doi.org/10.1186/s12951-017-0262-9.
Sharifi, F., Irani, S., Zandi, M., Soleimani, M., Atyabi, S. M., 2016. Comparative of fibroblast and osteoblast cells adhesion on surface modified nanofibrous substrates based on polycaprolactone. Prog Biomater. 5, 213-222. https://doi.org/10.1007/s40204-016-0059-1.
Shipp, D. W., Sinjab, F., Notingher, I., 2017. Raman spectroscopy: techniques and applications in the life sciences. Adv. Opt. Photonics. 9, 315-428 https://doi.org/10.1364/AOP.9.000315.
Shokrzadeh, M., Habibi, E., Modanloo, M., 2017. Cytotoxic and genotoxic studies of essential oil from Rosa damascene Mill., Kashan, Iran. Med Glas. 14, 152-157. http://doi.org/10.17392/901-17.
Schillaci, D., Napoli, E. M., Cusimano, M. G., Vitale, M., Ruberto, G., 2013. Origanum vulgare subsp. hirtum Essential Oil Prevented Biofilm Formation and Showed Antibacterial Activity against Planktonic and Sessile Bacterial Cells. J Food Prot. 76, 1747-1752 https://doi.org/10.4315/0362-028X.JFP-13-001.
Singh, N. P., McCoy, M. T., Tice, R. R., Schneider, E. L., 1988. A simple technique for quantitation of low levels of DNA damage in individual cells. Exp. Cell Res. 175, 184-191. https://doi.org/10.1016/0014-4827(88)90265-0.
Smith, R., Wright, K. L., Ashton, L., 2016. Raman spectroscopy: an evolving technique for live cell studies. Analyst. 141, 3590-3600. https://doi.org/10.1039/C6AN00152A.
Sohová, M. E., Bodík, M., Siffalovic, P., Bugárová, N., Labudová, M., Zaťovičová, M., ... Pastoreková, S., 2018. Label-free tracking of nanosized graphene oxide cellular uptake by confocal Raman microscopy. Analyst. 143, 3686-3692. https://doi.org/10.1039/C8AN00225H.
Takahashi, C., Akachi, Y., Ogawa, N., Moriguchi, K., Asaka, T., Tanemura, M., ... Yamamoto, H., 2017. Morphological study of efficacy of clarithromycin-loaded nanocarriers for treatment of biofilm infection disease. Med. Mol. Morphol. 50(1), 9-16. e https://doi.org/10.1007/s00795-016-0141-8
Torge, A., Wagner, S., Chaves, P. S., Oliveira, E. G., Guterres, S. S., Pohlmann, A. R., ... Beck, R. C., 2017. Ciprofloxacin-loaded lipid-core nanocapsules as mucus penetrating drug delivery system intended for the treatment of bacterial infections in cystic fibrosis. Int. J. Pharm. 527(1-2), 92-102. https://doi.org/10.1016/j.ijpharm.2017.05.013
Türeli, N. G., Torge, A., Juntke, J., Schwarz, B. C., Schneider-Daum, N., Türeli, A. E., ... Schneider, M., 2017. Ciprofloxacin-loaded PLGA nanoparticles against cystic fibrosis P. aeruginosa lung infections. Eur J Pharm Biopharm., 117, 363-371. https://doi.org/10.1016/j.ejpb.2017.04.032
Valeriano, C., De Oliveira, T. L. C., De Carvalho, S. M., das Graças Cardoso, M., Alves, E., Piccoli, R. H., 2012. The sanitizing action of essential oil-based solutions against

782 Salmonella enterica serotype Enteritidis S64 biofilm formation on AISI 304 stainless
783 steel. Food Control. 25, 673-677. https://doi.org/10.1016/j.foodcont.2011.12.015.
784 Weiss, J., Gaysinsky, S., Davidson, M., McClements, J., 2009. CHAPTER 24 -
785 Nanostructured Encapsulation Systems: Food Antimicrobials. Global issues in food
786 science and technology. Academic Press, 425-479. https://doi.org/10.1016/B978-0-12-
787 374124-0.00024-7.
788 Woodruff, M. A., Hutmacher, D. W., 2010. The return of a forgotten polymer—
789 Polycaprolactone in the 21st century. Prog. Polym. Sci. 35, 1217-1256.
790 https://doi.org/10.1016/j.progpolymsci.2010.04.002.
791 Zijno, A., De Angelis, I., De Berardis, B., Andreoli, C., Russo, M. T., Pietraforte, D., ...
792 Barone, F., 2015. Different mechanisms are involved in oxidative DNA damage and
793 genotoxicity induction by ZnO and TiO2 nanoparticles in human colon carcinoma
794 cells. Toxicol. In Vitro. 29, 1503-1512. https://doi.org/10.1016/j.tiv.2015.06.009.
795

Table 1: MIC, MBC and MFC values of encapsulated essential oils with respect to pure essential oils against *S. aureus*, *E. coli* and *C. albicans*.

Strain	Th-NC		Or-NC		Th-EO		Or-EO	
	MIC	MBC/MFC	MIC	MBC/MFC	MIC	MBC/MFC	MIC	MBC/MFC
S. aureus	0.5	1	0.5	1	2	3	1	2
E. coli	0.125	0.25	0.125	0.25	2	3	2	3
C. albicans	0.125	0.25	0.125	0.25	1	2	1	2

*MIC, MBC and MFC are expressed in mg/mL of essential oil

Figure captions:

Figure 1. Effect of NCs, EO-NCs, EOs on viable cells of *S. aureus* (A), *E. coli* (B), *C. albicans* (C) in the biofilm. Notes.**p<0.01.***p<0.001 indicate statistically significant differences compared to each control treatment without test substances (Student'st-test).

Figure 2. Cytotoxicity/viability of HaCaT cells treated with NCs, EO-NCs, EOs (0.00–2.08 mg/mL) for 24 h.

Figure 3. The levels of DNA single strand breaks (% of tail DNA) in HaCaT cells after the exposure to NCs, EO-NCs, EOs for 24 h. Data represent means ± SD of three independent experiments. Positive control - hydrogen peroxide (300 µmol/l).

Figure 4. CRM imaging of HaCaT cells after 24 h incubation with Th-NCs (0.1 mg/mL) and Or-NCs (0.0219 mg/mL). The red squares on bright field images display the scanned areas. The false-colored images present the results after PCA and cluster analysis. In some cases the corresponding Raman spectra are showed.

Figure 5. CRM imaging of HaCaT cells after 24 h incubation with Th-NCs (0.004 mg/mL) and Or-NCs (0.00219 mg/mL), and imaging of control HaCaT cells without additives. The red squares on bright field images display the scanned areas. The false-colored images and corresponding Raman spectra obtained after cluster analysis are presented.

Figure 6. False-colored images as a result of cluster analysis of hyperspectral Raman images of HaCaT cells after 24 h incubation with NCs (0.0468 mg/mL), Th-EO (0.1 mg/mL) and Or-EO (0.088 mg/mL).

A

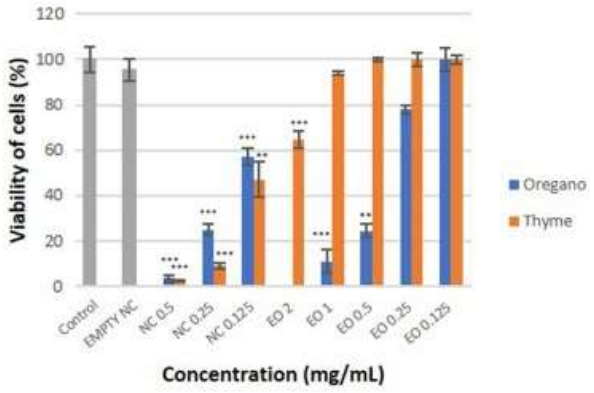
120
100
80
60
40
20
0
Viability of cells (%)
Control
EMPTY NC
NC 0.5
NC 0.25
NC 0.125
EO 2
EO 1
EO 0.5
EO 0.25
EO 0.125
Concentration (mg/mL)
Oregano
Thyme

B

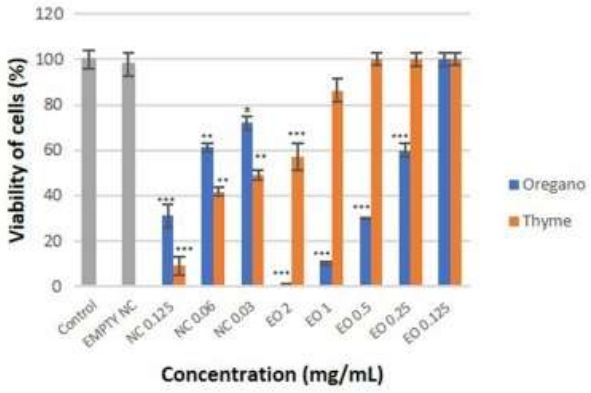
120
100
80
60
40
20
0
Viability of cells (%)
Control
EMPTY NC
NC 0.125
NC 0.06
NC 0.03
EO 2
EO 1
EO 0.5
EO 0.25
EO 0.125
Concentration (mg/mL)
Oregano
Thyme

C

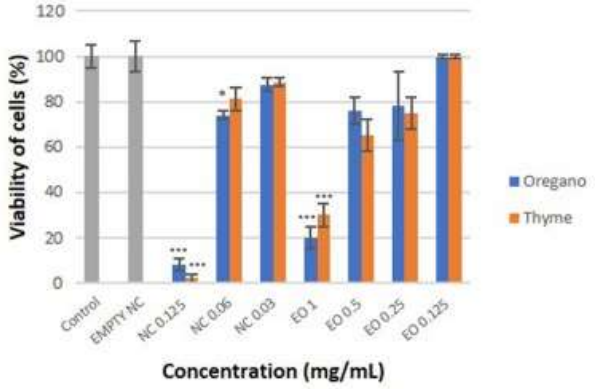
120
100
80
60
40
20
0
Viability of cells (%)
Control
EMPTY NC
NC 0.125
NC 0.06
NC 0.03
EO 1
EO 0.5
EO 0.25
EO 0.125
Concentration (mg/mL)
Oregano
Thyme

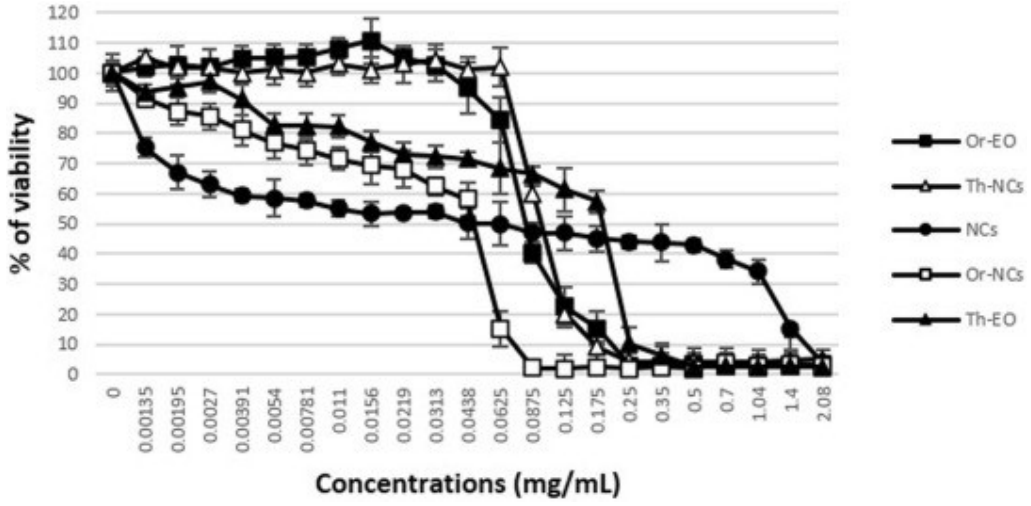
120
110
100
90
80
70
60
50
40
30
20
10
0
% of viability
0
0.00135
0.00195
0.0027
0.00391
0.0054
0.00781
0.011
0.0156
0.0219
0.0313
0.0438
0.0625
0.0875
0.125
0.175
0.25
0.35
0.5
0.7
1.04
1.4
2.08
Concentrations (mg/mL)
Or-EO
Th-NCs
NCs
Or-NCs
Th-EO

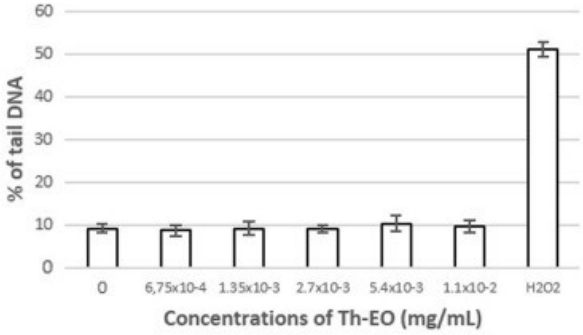
60
50
40
30
20
10
0
% of tail DNA
0
6,75x10-4
1.35x10-3
2.7x10-3
5.4x10-3
1.1x10-2
H2O2
Concentrations of Th-EO (mg/mL)

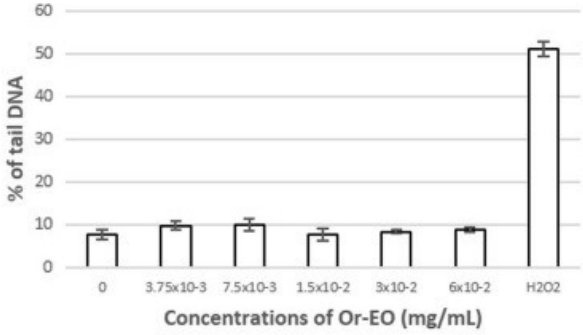
60
50
40
30
20
10
0
% of tail DNA
0
3.75x10-3
7.5x10-3
1.5x10-2
3x10-2
6x10-2
H2O2
Concentrations of Or-EO (mg/mL)

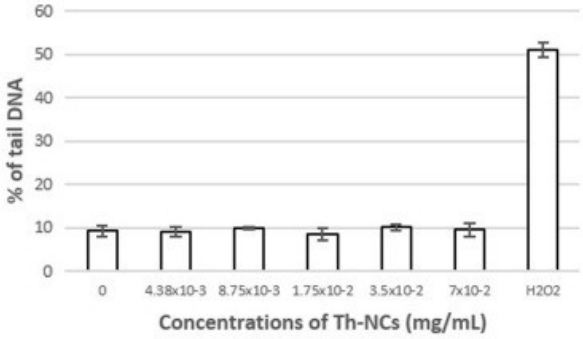
60
50
40
30
20
10
0
% of tail DNA
0
4.38x10-3
8.75x10-3
1.75x10-2
3.5x10-2
7x10-2
H2O2
Concentrations of Th-NCs (mg/mL)

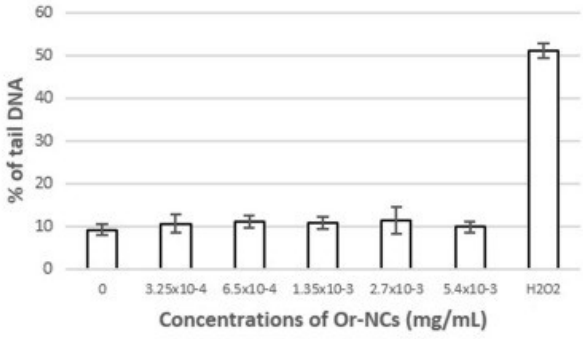
60
50
40
30
20
10
0
% of tail DNA
0
3.25x10-4
6.5x10-4
1.35x10-3
2.7x10-3
5.4x10-3
H2O2
Concentrations of Or-NCs (mg/mL)

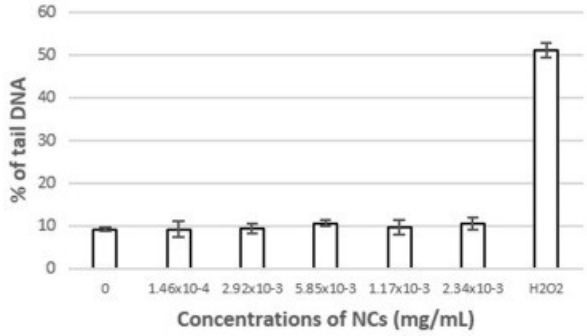
60
50
40
30
20
10
0
% of tail DNA
0
1.46x10-4
2.92x10-3
5.85x10-3
1.17x10-3
2.34x10-3
H2O2
Concentrations of NCs (mg/mL)

Cells after incubation with Th-NCs (high conc.)

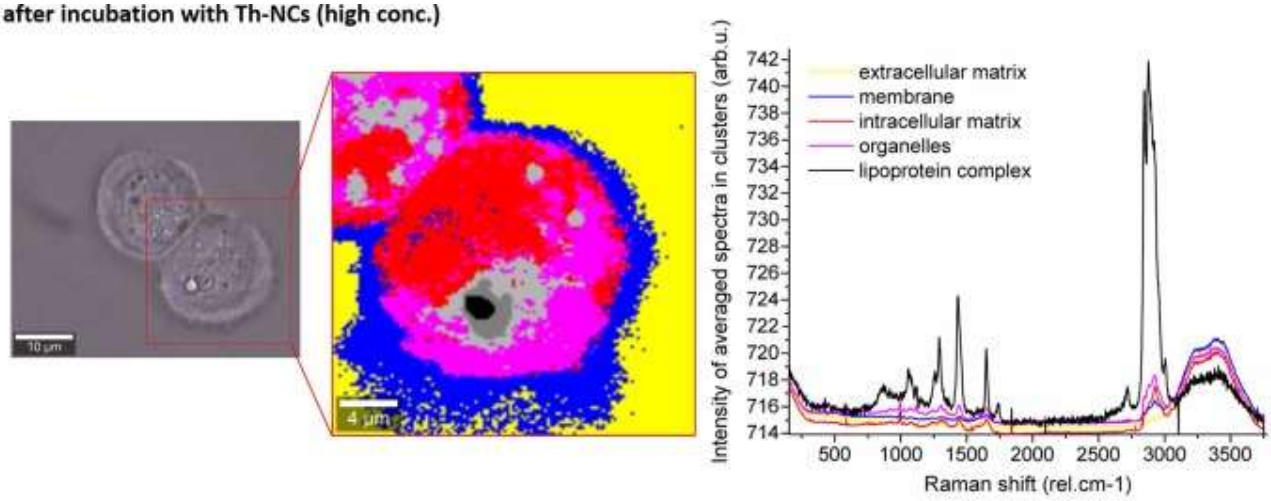

Example of a z-scan at different focal depths:

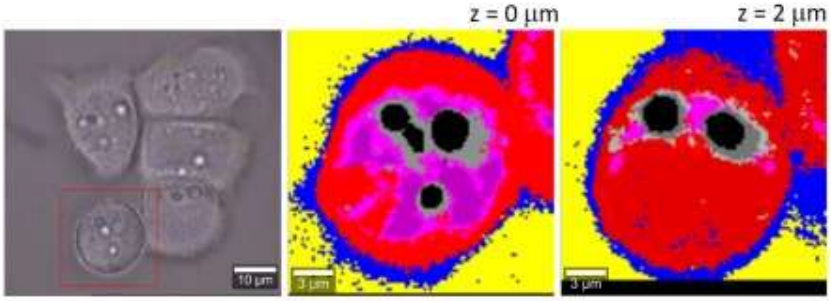

Cells after incubation with Or-NCs (high conc.)

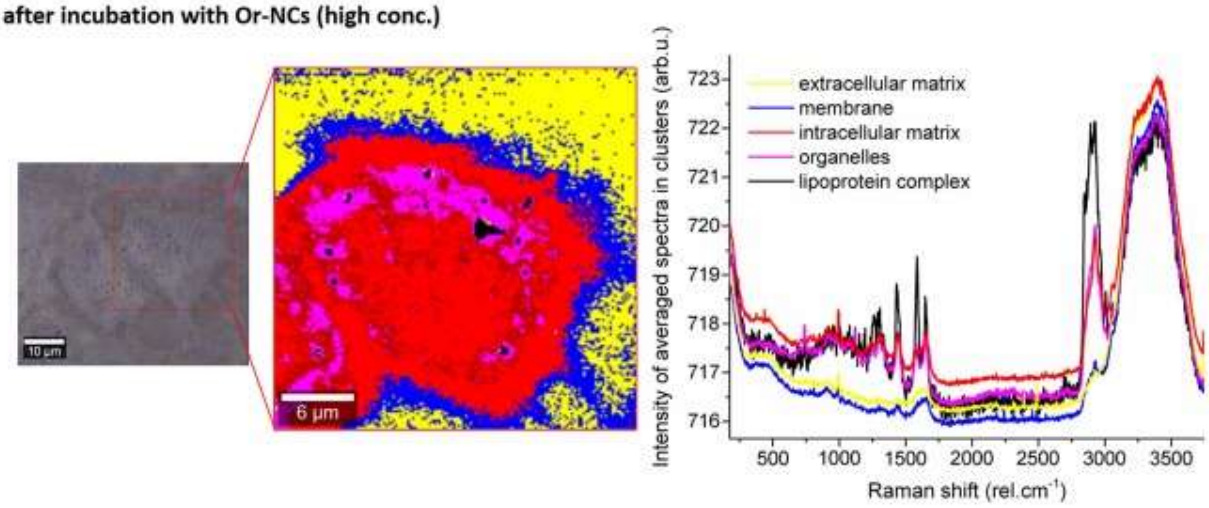

Other examples:

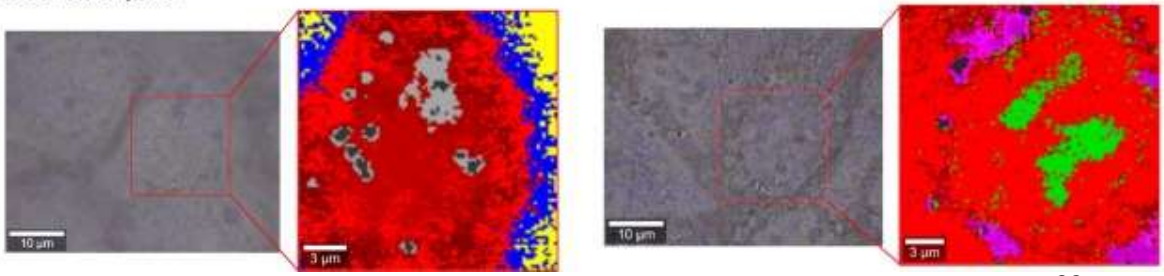

Cells after incubation with Th-NCs (low conc.)

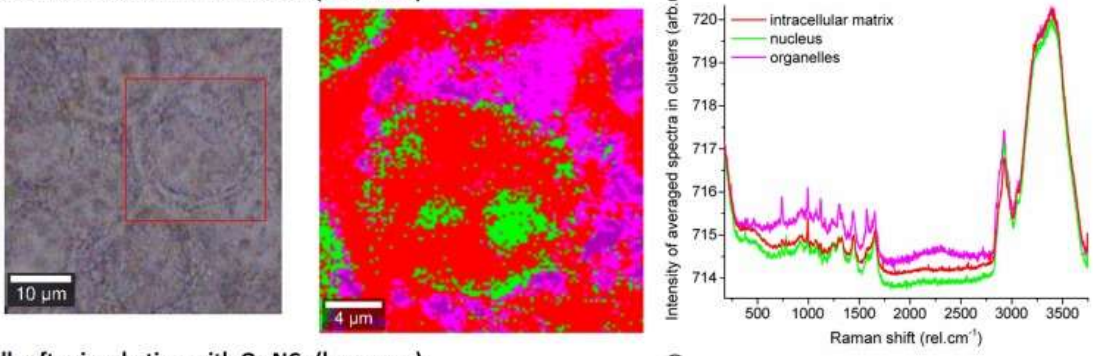

Cells after incubation with Or-NCs (low conc.)

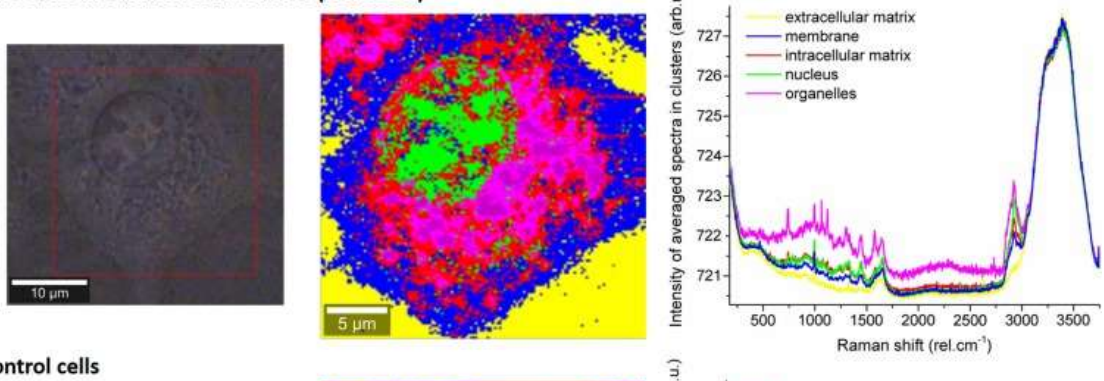

Control cells

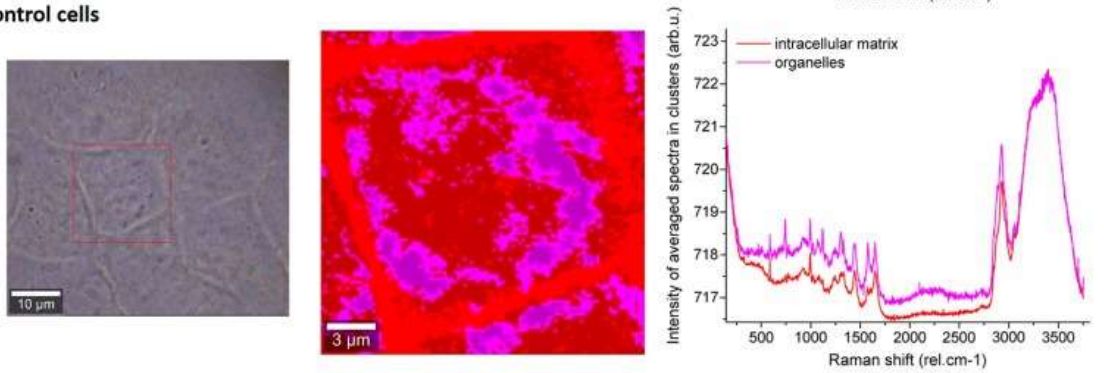

Cells after incubation with NCs (high conc.)

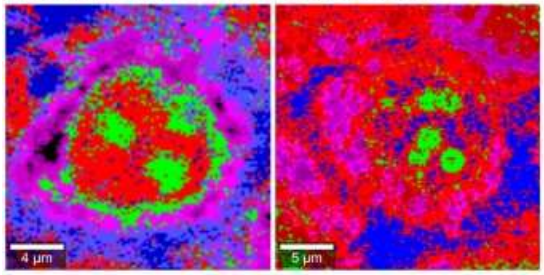

Cells after incubation with Th-EO (high conc.)

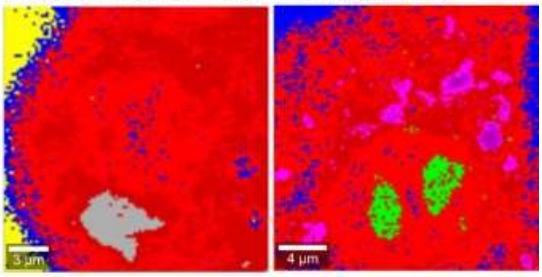

Cells after incubation with Or-EO (high conc.)